UCRL-17217

University of California

Ernest O. Lawrence Radiation Laboratory

STRANGE-PARTICLE PRODUCTION IN $\pi^- p$ INTERACTIONS FROM 1.5 TO 4.2 BeV/c
PART II. TWO-BODY FINAL STATES

Berkeley, California

DISCLAIMER

Submitted to the Physical Review

UCRL-17217
Preprint

UNIVERSITY OF CALIFORNIA

Lawrence Radiation Laboratory
Berkeley, California

AEC Contract No. W-7405-eng-48

STRANGE-PARTICLE PRODUCTION IN π^-p INTERACTIONS FROM 1.5 TO 4.2 BeV/c

PART II. TWO-BODY FINAL STATES

Orin I. Dahl, Lyndon M. Hardy, Richard I. Hess
Janos Kirz, Donald H. Miller, and Joseph A. Schwartz

January 1967

Strange-Particle Production in π^-p Interactions from 1.5 to 4.2 BeV/c

Part II. Two-Body Final States*

Orin I. Dahl, Lyndon M. Hardy,† Richard I. Hess,‡ Janos Kirz, Donald H. Miller, and Joseph A. Schwartz§

Department of Physics and Lawrence Radiation Laboratory
University of California, Berkeley, California

January 1967

ABSTRACT

The reactions $\pi^-p \to \Lambda K^0$, $\Sigma^0 K^0$, and $\Sigma^- K^+$ are studied in the 1.5 to 4.2-BeV/c momentum range.

Total cross sections, angular distributions, and the polarization of the Λ in the ΛK^0 channel are presented. The dominant features of the reactions are parametrized in terms of meson- and baryon-exchange contributions.

I. INTRODUCTION

Numerous authors have reported results on the associated production reactions

$$\pi^- p \rightarrow \Lambda K^0 \quad (1)$$

$$\Sigma^0 K^0 \quad (2)$$

$$\Sigma^- K^+ \quad (3)$$

at energies from threshold to 1.5 BeV/c.[1] This work is an extension of these studies into the energy range 1.5 to 4.2 BeV/c. Recently experiments have also been performed in this momentum range[2-7] and at higher energies.[8-11]

This experiment was performed at the Bevatron with the 72-in. bubble chamber. The experimental procedure, and results on three-and-more-body final states are reported in the preceding paper.[12] We refer the reader to that paper for details on the analysis of the data. Here we discuss only those features relevant to the two-body final states ΛK^0, $\Sigma^0 K^0$, and $\Sigma^- K^+$.

Our sample, based on 890 000 pictures, consists of 4300 ΛK^0 events, 1200 $\Sigma^0 K^0$ events, and 2600 $\Sigma^- K^+$ events. This sample satisfies the following selection criteria: For the ΛK^0 final state we use events for which either $\Lambda \rightarrow p\pi^-$ or $K^0 \rightarrow \pi^+\pi^-$ or both decays are observed within the fiducial volume. For the $\Sigma^0 K^0$ final state we require that $K^0 \rightarrow \pi^+\pi^-$ be observed. For the $\Sigma^- K^+$ final state we require that $\Sigma^- \rightarrow n\pi^-$ decay be observed. In each case we demand a distance of at least 0.5 cm between production and decay vertices. Each event is weighted by the reciprocal of the probablity that the above requirements are met.

Once the consistency of the kinematic fits with bubble density is verified on the scan table, reaction (3) is well enough constrained that the

sample is essentially uncontaminated. The same holds true for reactions (1) and (2) if both the Λ and K^0 decays are observed. If only one decay is observed, assignment of events is based on missing-mass selection criteria.[13] By reprocessing the well-constrained two-decay events as if only one decay were observed, we found that the cross contamination between the Λ and Σ^0 channels for the whole sample is less than 10% at all beam momenta.

II. TOTAL CROSS SECTIONS

For cross section measurements only, the experiment was divided into two parts. Results on the first part (π72) have been given by Schwartz,[14] and are merely quoted here. In this case, the total number of interactions was estimated from a scan of every fifth frame in a randomly chosen sample of film; frames with more than 22 tracks (TMT's) were treated separately. A sample of 270 TMT's was scanned, yielding a mean of 28.3 tracks/TMT; the total number of interactions at each beam momentum was prorated accordingly. Corrections of +2±2% for scanning efficiency, and -2.5% for events falling outside the fiducial volume were applied; the path length corresponding to the total number of interactions at each momentum was calculated using the cross section values reported by Diddens et al.[15]

In the second part (π63) a selected sample of film was scanned completely for all interactions in each momentum interval. The number of observed two-prong events was corrected by +10±3% to account for unnoticed small-angle scatterings. Using the information from this special scan, and with the data of Diddens et al.[15] and Citron et al.,[16] we determined the cross section per event found in the general scan. Final cross sections were determined by comparing the corrected number of fitted events of a given type with the corresponding number of events found in the general scan.

This procedure is described in detail in the preceding paper.[12]

Since cross-section determinations were not identical, there may be small systematic differences in the two parts of the experiment. Our results, as well as those of other experiments[2-8] are presented in Table I. In Fig. 1 the same data are plotted on a log-log scale as a function of total c.m. energy, $E_{c.m.}$. In each case the cross section decreases monotonically with increasing energy. Since the data in Fig. 1 lie essentially on three straight lines, they have been fitted to

$$\sigma_T = A(E_{c.m.})^B. \qquad (4)$$

This expression provides adequate fits to reactions (2) and (3). For the $\Sigma^0 K^0$ final state, the least-squares fit gives $B = -3.30 \pm 0.30$, with $\chi^2 = 24.6$ for 24 data points. For the $\Sigma^- K^+$ final state, we have $B = -9.30 \pm 0.25$ with $\chi^2 = 34.5$ for 25 data points. For the ΛK^0 final state, we have $B = -3.57 \pm 0.20$ with $\chi^2 = 60.1$ for 25 data points; consequently, in this case the fit is poor.

We have considered the possibility that the poor fit in the ΛK^0 channel reflects a significant contribution to the cross section from s-channel resonances. It is not difficult to see that a better fit to $\sigma_T(\Lambda K^0)$ in Fig. 1 may be obtained with a linear "background" and a peak superimposed near $E_{c.m.} \cong 2200$ MeV. It appears reasonable to identify this with $N^*_{1/2}(2190)$; however, most data with $E_{c.m.} < 2350$ MeV represent (π72), while most data with $E_{c.m.} > 2350$ MeV were obtained in (π63). Consequently, possible systematic differences in normalization are crucial. Should the peak represent a contribution from decay of $N^*_{1/2}(2190)$, characteristic structure will appear in angular distributions and polarizations, these considerations are discussed further in Sections III and IV.

Recently, Morrison pointed out the existence of strong regularities in the energy dependences of cross sections for a large number of reactions.[17] By fitting measured cross sections to the expression

$$\sigma_T = C\left(\frac{p_{in}}{p_0}\right)^{-n} , \qquad (5)$$

where p_{in} is the beam momentum in the laboratory system and p_0 is a constant, he found that values of the exponent n fall into at least three distinct groups. When the reaction can be interpreted as exchange of a non-strange meson, $n \simeq 1.5$; when the reaction involves exchange of a strange meson, $n \simeq 2.0$; when the reaction occurs through baryon exchange, $n \simeq 4.0$.

For comparison, the data in the present experiment have been fitted to expression (5). We find that $n = 1.45 \pm 0.08$ for $\pi^- p \rightarrow \Lambda K^0$; $n = 1.36 \pm 0.13$ for $\pi^- p \rightarrow \Sigma^0 K^0$; and $n = 3.78 \pm 0.10$ for $\pi^- p \rightarrow \Sigma^- K^+$. Since the isotopic spin is 1/2 for all presently known strange mesons, it is likely that only the ΛK^0 and $\Sigma^0 K^0$ final states can be produced through single-meson exchange. For the $\Sigma^- K^+$ final state, the simplest production mechanism involves baryon exchange. Consequently the observed n values are roughly consistent with the pattern suggested by Morrison; however, over the energy range studied they do not support the distinction between reactions involving exchange of strange and nonstrange mesons.

III. DIFFERENTIAL CROSS SECTIONS

For the analysis of differential cross sections the data were divided into 11 momentum bins centered at $p_{in} = 1.50$, 1.60, 1.70, 1.86, 1.95, 2.05, 2.20, 2.35, 2.60, 3.15, and 4.0 BeV/c. For the first nine bins, Δp_{in} is ± 50 MeV/c; for the bins centered at $p_{in} = 3.15$ and 4.0 BeV/c, events were accepted with

$2.9 \leq p_{in} \leq 3.3$ BeV/c and $3.8 \leq p_{in} \leq 4.2$ BeV/c, respectively.

The results are summarized in Table II, and are plotted in Figs. 2 to 4. The dotted curves represent least-squares fits to

$$\frac{d\sigma}{d\Omega} = \sum_n A_n P_n (\cos\theta), \tag{6}$$

where P_n are Legendre polynomials, and θ is the c.m. production angle;[18] the fitted coefficients A_n are given in Table III.

The dominant characteristics of the angular distributions are: (a) sharp peaking near $\cos\theta = +1$ for both the ΛK^0 and $\Sigma^0 K^0$ channels which may be mediated by single-meson exchange; (b) peaking near $\cos\theta = -1$ for the $\Sigma^- K^+$ channel which can occur only through baryon exchange; and (c) the smaller peak near $\cos\theta = -1$ for the ΛK^0 channel. We discuss each of these features in turn.

Rather than use $\cos\theta$, it is convenient to introduce the square of the four-momentum-transfer

$$t = (E_Y - E_p)^2 - (\underset{\sim}{p}_Y - \underset{\sim}{p}_p)^2 \tag{7}$$

which is Lorentz invariant. In the c.m. system $dt = 2p_Y p_p \, d(\cos\theta)$. The maximum value, t_0, occurs at $\cos\theta = +1$. The distributions in $t_0 - t$ are shown in Fig. 5 for the ΛK^0 and $\Sigma^0 K^0$ final states. The lines represent maximum-likelihood fits to the expression

$$\frac{d\sigma}{dt} = C \exp[-D(t_0 - t)] \tag{8}$$

over the region $0 \leq t_0 - t \leq 0.4$ $(\text{BeV/c})^2$. Over the energy range covered in this experiment, secondary maxima in the differential cross sections are significant. When a wider interval of momentum transfer is included in the fit, the slope, D, changes beyond the range of errors. Consequently, the fit shown in Fig. 5 must be considered qualitative.[19]

To explore further the connection between the Legendre and the exponential fits, expression (8) was expanded in Legendre polynomials.[20] For this calculation we set D equal to $7(\text{BeV}/c)^{-2}$; to avoid problems of normalization, the ratios A_n/A_0 for each beam momentum were compared with the corresponding fitted quantities from Table III. On Fig. 6 this comparison is shown for the ΛK^0 final state. Clearly, for the low-order coefficients ($n \leq 5$), the expansion gives consistently larger values of A_n/A_0 than the fit to the differential cross section. For the high-order coefficients ($n \geq 6$), however, the agreement in size and energy dependence is remarkably good. This suggests, that the appearance of higher partial waves is dictated by the peripheral peak alone.

In the presence of an s-channel resonance strongly coupled to the ΛK^0 system, it may be expected that the coefficients A_n/A_0 will vary rapidly in the neighborhood of the resonance. The behavior of all coefficients shown on Fig. 6 is smooth; consequently the data show no evidence for any s-channel resonance. In particular we find no evidence for the process $\pi^- p \rightarrow N^*(2190) \rightarrow \Lambda K^0$.

The $\Sigma^- K^+$ final state, in contrast to ΛK^0 and $\Sigma^0 K^0$ shows no peripheral peaking. What one observes is rather an "antiperipheral" peak, near $\cos\theta = -1$. This behavior follows the pattern of other reactions such as $K^- p \rightarrow \Xi^- K^+$, where the t channel quantum numbers require the exchange of an $I = 3/2$ strange meson. It is therefore plausible to assume that the dominant contribution to the reaction arises from baryon exchange in the u channel.[21] Among the known baryons those with $I = 0$ or 1 can contribute in the $\Sigma^- K^+$ reaction. However, the lack of "antiperipheral" peaking in the $\Sigma^0 K^0$ case, where only $I = 1$ baryons could be exchanged, suggests the dominance of $I = 0$ exchange.[22]

In analogy with Eq. (7) we define the Lorentz-invariant four-momentum transfer squared in the u channel as

$$u = (E_K - E_p)^2 - (\underline{p}_K - \underline{p}_p)^2. \qquad (9)$$

In the c.m. system we have $du = -2p_K p_p d(\cos\theta)$. The maximum value, u_0, occurs when $\cos\theta = -1$. The distribution in $u_0 - u$ is presented on Fig. 7. The line superimposed on the data represents a maximum-likelihood fit to the expression

$$\frac{d\sigma}{du} = C \exp[-D(u_0 - u)] \qquad (10)$$

in the region $0 \leq u_0 - u < 1 (\mathrm{BeV}/c)^2$.

The $\Sigma^- K^+$ channel also differs from ΛK^0 and $\Sigma^0 K^0$ in the simplicity of its production angular distribution. The Legendre-polynomial fit is in reasonable agreement with the expansion of expression (10), [with $D = 1.4$ $(\mathrm{BeV}/c)^{-2}$] above 2.2 BeV/c. This behavior suggests that the interaction volume is considerably smaller for $\pi^- p \to \Sigma^- K^+$ than for $\pi^- p \to \Lambda K^0$, $\Sigma^0 K^0$, or most other reactions. Below 2.2 BeV/c the fit to Legendre polynomials up to second order is adequate. To remove the dependence on the total cross section, we divide by A_0, and present the ratios A_1/A_0 and A_2/A_0 on Fig. 8. It is interesting to note that the fitted coefficients A_1 and A_2 go through marked variations near 1.9 BeV/c. We have no explanation for the observed behavior.

The "antiperipheral" peak in the ΛK^0 final state can also be considered in terms of a baryon-exchange model. Here, as in the $\Sigma^0 K^0$ case, only hyperons with $I = 1$ can contribute in the u channel.[23] In Fig. 9 we present the $d\sigma/du$ distribution in the 2-BeV/c region only. At higher energies the number of events near $\cos\theta = -1$ is too small to give a meaningful spectrum.

We fitted the energy dependence of the differential cross section at constant momentum transfer to the expression

$$\frac{d\sigma}{dt} = F \quad (E_{c.m.})^m \qquad (11)$$

in the region of the peripheral peaks. For the antiperipheral peaks we fitted $d\sigma/du$ to an expression of the same form. Results of the fit are presented in Table IV. We note that:

(a) the values of the exponent m found for the ΛK^0 and $\Sigma^0 K^0$ data are similar for the peripheral peak;

(b) the values of m found for the ΛK^0 and $\Sigma^- K^+$ data are similar for the antiperipheral peak;

(c) the cross sections fall faster at larger momentum transfer. This "shrinking" of the peaks may indicate some Regge-type behavior.

The data presented allow us to make a few comments concerning the reaction $\pi^+ p \to \Sigma^+ K^+$ in the 3- to 4-BeV/c range. We use the relation between the complex amplitudes A^+, A^0, and A^- for the reactions $\pi^+ p \to \Sigma^+ K^+$, $\pi^- p \to \Sigma^0 K^0$, and $\pi^- p \to \Sigma^- K^+$, respectively. Charge independence predicts

$$A^- + \sqrt{2} A^0 = A^+. \qquad (12)$$

Near $\cos\theta = +1$ the cross section for the $\Sigma^- K^+$ reaction is much smaller than that for $\Sigma^0 K^0$, and therefore A^- is small compared to A^0 (A^0 is small compared to A^- near $\cos\theta = -1$). In a first approximation we neglect the small amplitude, to obtain $(d\sigma/d\Omega)_{\Sigma^+ K^+} \approx 2(d\sigma/d\Omega)_{\Sigma^0 K^0}$ near $\cos\theta = +1$, and since the total cross section is dominated by the peripheral peak, we have $(\sigma_T)_{\Sigma^+ K^+} \sim 2(\sigma_T)_{\Sigma^0 K^0}$ above 3 BeV/c. In the same way we find that $(d\sigma/d\Omega)_{\Sigma^+ K^+}$ will have a small peak of the same order of magnitude as $(d\sigma/d\Omega)_{\Sigma^- K^+}$ near $\cos\theta = -1$.[24]

IV. POLARIZATION

For the reaction $\pi^- p \to \Lambda K^0$ the $\Lambda \to p\pi^-$ decay is a good analyzer of the Λ polarization. The angular distribution of the decay proton with respect to the production normal $\underset{\sim}{n} = \underset{\sim}{p}_{\text{beam}} \times \underset{\sim}{p}_{K^0}$ is of the form $(1 + \alpha_\Lambda \mathbb{P} \cos\xi)$, where $\alpha_\Lambda = 0.66$ is the asymmetry parameter, $\mathbb{P}$ is the polarization, and ξ is the angle between the momentum of the decay proton and $\underset{\sim}{n}$ in the Λ rest frame. The product of the differential cross section and the polarization at the production angle θ is given by

$$\alpha_\Lambda \mathbb{P}(\theta) \frac{d\sigma}{d\Omega} = 3c \sum_i \cos\xi_i ,$$

where the sum is over the events within an interval of the production angle,[25] and the constant c converts this sum into cross section units.

The results are presented in Fig. 10 and Table V. The curves on Fig. 10 represent least-squares fits to the form[18]

$$\alpha_\Lambda \mathbb{P}(\theta) \frac{d\sigma}{d\Omega} = \sin\theta \sum_n B_n \frac{dP_{n+1}(\cos\theta)}{d(\cos\theta)} ,$$

where P_n is the nth-order Legendre polynomial. The fitted coefficients B_n are shown in Table VI. In Fig. 11 we present the polarization as a function of the momentum transfer. The size and shape of the distribution are similar for the data near 2 and 3 BeV/c.[26] We find the polarization positive at low momentum transfer, then negative in the region $t - t_0 \approx -1$ (BeV/c)^2. The cross-over point is near $t - t_0 = -0.5$ (BeV/c)^2. The largest negative value of the polarization remains consistent with 100% even at the highest beam momenta.

We note that the simplest one-particle and one-Regge-pole exchange models predict no polarization for the final-state hyperon. Using a model

based on the exchange of both the $K^*(890)$ and $K^*(1410)$ Regge trajectories, Sarma and Reeder[27] successfully fitted both the angular distribution and the Σ^+ polarization in the reaction $\pi^+ p \to \Sigma^+ K^+$ at 3.23 BeV/c.[24] Since the qualitative features of the $\Sigma^+ K^+$ channel are strikingly similar to the data presented here, extention of their analysis to include the ΛK^0 final state seems highly desirable.[28]

Due to lack of statistics in Σ^0 and to the small value of the asymmetry parameter in Σ^- decay, we have no significant results on Σ polarization.[29]

V. SUMMARY AND ACKNOWLEDGMENTS

In summary, we find that the dominant features of the reactions $\pi^- p \to \Lambda K^0$, $\Sigma^0 K^0$, and $\Sigma^- K^+$ can be described in terms of meson and baryon exchange in the t and u channels, respectively. All cross sections decrease with increasing beam momentum, more slowly for meson exchange than for baryon exchange. The polarization of the Λ in $\pi^- p \to \Lambda K^0$ remains large in the region of moderate momentum transfer [$|t| \leq 1 (\text{BeV}/c)^2$], even at the highest energies available in this experiment.

The energy dependence of the total cross sections and the momentum-transfer distribution is suggestive of Regge-type behavior. In terms of the Regge picture the observed polarization requires that two K^* trajectories contribute to $\pi^- p \to \Lambda K^0$.

The results presented indicate a break in the peripheral peaks near $t - t_0 \approx -0.5 (\text{BeV}/c)^2$ and a change of sign of the Λ polarization at about the same value of the momentum transfer. Similar phenomena observed in several other reactions[24, 30] have been associated with the passage of the exchanged Regge trajectories through zero.[19, 27]

We wish to thank the scanning and measuring staff for their untiring efforts, and members of the Bevatron and bubble-chamber operations groups for the excellent cooperation we received at the time of the exposure. Drs. Gideon Alexander, George R. Kalbfleisch, and Gerald A. Smith have participated in the analysis of the first stages of the experiment. We are grateful to Professor David Jackson for helpful comments. It is a pleasure to thank Professor Luis W. Alvarez for his encouragement and support, and members of the Alvarez Group for their help and criticism.

FOOTNOTES AND REFERENCES

* This work was done under the auspices of the U. S. Atomic Energy Commission. Part of this paper is from a thesis submitted by J. A. Schwartz to the Graduate Division of the University of California, Berkeley, California in partial fulfillment of the requirements for the degree of Doctor of Philosophy.

† Present address: TRW Systems, Inc., 1 Space Park, Redondo Beach, California.

‡ Present address: Logicon, Inc., 205 Avenue I, Redondo Beach, California.

§ Present address: College of Physicians and Surgeons, Columbia University, 722 W. 168 St., New York, N. Y.

1. Some of the reports on strange-particle production up to 1.5 BeV/c are:

(a) L. Bertanza, P. L. Connolly, B. B. Culwick, F. R. Eisler, T. Morris, R. Palmer, A. Prodell, and N. P. Samios, Phys. Rev. Letters 8, 332 (1962) (900, 920, 960, and 1000 MeV/c);

(b) F. S. Crawford, Jr., M. Cresti, R. L. Douglass, M. L. Good, G. R. Kalbfleisch, M. L. Stevenson, H. K. Ticho, in Ninth Annual International Conference on High Energy Physics, Kiev, 1959 [Academy of Science (IUPAP), Moscow, Russia, 1960), Vol. 1, p. 443 (940 to 1220 MeV/c);

(c) Joseph Keren, Phys. Rev. 133, B457 (1964) (1020 MeV/c);

(d) J. A. Anderson, F. S. Crawford, B. B. Crawford, R. L. Golden, L. J. Lloyd, G. W. Meisner, and L. R. Price, in Proceedings of the 1962 Annual International Conference on High Energy Physics at CERN (CERN, Geneva, 1962), p. 270 (1035, 1220 MeV/c);

(e) F. Eisler, R. Plano, A. Prodell, N. Samios, M. Schwartz, J. Steinberger, P. Bassi, V. Borelli, G. Puppi, G. Tanaka, P. Waloschek, V. Zoboli, M. Conversi, P. Franzini, I. Mannelli, R. Santangelo, V. Silverstrini, D. A. Glaser, C. Graves, M. L. Perl, Phys. Rev. 108, 1353 (1957) (1040, 1080, and 1230 MeV/c);
Also Nuovo Cimento 10, 468 (1958) (1040, 1090, 1330, 1430 MeV/c);

(f) L. B. Leipuner and R. K. Adair, Phys. Rev. 109, 1358 (1958) (1090 MeV/c);

(g) Y. S. Kim, G. R. Burleson, P. I. P. Kalmus, A. Roberts, C. L. Sandler, and T. A. Romanowski, Phys. Rev. 151, 1090 (1966) (1.17, 1.32 BeV/c);

(h) F. S. Crawford, Jr., M. Cresti, M. L. Good, K. Gottstein, E. M. Lyman, F. T. Solmitz, M. L. Stevenson, and H. K. Ticho, in Proceedings of the 1958 Annual International Conference on High Energy Physics at CERN (CERN, Geneva, 1958), p. 323 (1120 MeV/c);

(i) J. A. Anderson (Ph. D. Thesis), Lawrence Radiation Laboratory Report UCRL-10838, May 27, 1963 (unpublished)(1170 MeV/c);

(j) F. S. Crawford, Jr., R. L. Douglas, M. L. Good, G. R. Kalbfleisch, M. L. Stevenson, and H. K. Ticho, Phys. Rev. Letters 3, 394 (1959) (1220 MeV/c);

(k) J. L. Brown, D. A. Glaser, D. I. Meyer, M. L. Perl, J. Vander Velde, and J. W. Cronin, Phys. Rev. 107, 906 (1957); and J. L. Brown, D. A. Glaser, and M. L. Perl, Phys. Rev. 108, 1036 (1957) (1230 MeV/c).

2. L. L. Yoder, C. T. Coffin, D. I. Meyer, and K. M. Terwilliger, Phys. Rev. 132, 1778 (1963) (1508 MeV/c).

3. O. Goussu, M. Sené, B. Ghidini, S. Mongelli, A. Romano, P. Waloschek, and V. Alles-Borelli, Nuovo Cimento 42, A606 (1966) (1.59 BeV/c).

4. D. H. Miller, A. Z. Kovacs, R. McIlwain, T. L. Palfrey, and G. W. Tautfest, Phys. Rev. 140, B360 (1965) (2.7 BeV/c).

5. O. Goussu, G. Smadja, and G. Kayas, Nuovo Cimento (to be published) (2.75 BeV/c).

6. T. P. Wangler, A. R. Erwin, and W. D. Walker, Phys. Rev. 137, B414 (1965) (3.0 BeV/c).

7. J. Bartsch et al., Aachen, Hamburg, London, München collaboration, Nuovo Cimento 43, A1010 (1966) (4.0 BeV/c).

8. L. Bertanza, B. B. Culwick, K. W. Lai, I. S. Mittra, N. P. Samios, A. M. Thorndike, S. S. Yamamoto, and R. M. Lea, Phys. Rev. 130, 786 (1963) (4.65 BeV/c).

9. V. A. Belyakov, V. I. Veksler, N. M. Viryasov, E. N. Kladnitskaya, G. I. Kopylov, V. N. Penev, and M. I. Solov'ev, J. Nucl. Phys. (USSR) 1, 240 and 249 (1966) (7.5 BeV/c).

10. R. Ehrlich, W. Selove, and H. Yuta, Phys. Rev. 152, 1194 (1966) (7.91 BeV/c).

11. A. Bigi, S. Brandt, A. deMarco-Trabucco, Ch. Peyrou, R. Sosnowski, and A. Wroblewski, Nuovo Cimento 33, 1249 (1964) (10 BeV/c).

12. O. I. Dahl, L. M. Hardy, R. I. Hess, J. Kirz, and D. H. Miller, Phys. Rev., (preceding paper); Lawrence Radiation Laboratory Report UCRL-16978, January 1967 (unpublished).

13. If only a $K^0 \rightarrow \pi^+\pi^-$ decay is seen, the event is admitted to the sample if the square of the missing mass is 1.15 $(BeV)^2 < MM^2 < 1.56$ $(BeV)^2$. If only a $\Lambda \rightarrow p\pi^-$ decay is seen, the limits are 0.2 $(BeV)^2 < MM^2 < 0.3$ $(BeV)^2$. Cross section values are corrected for the loss of events due to these cuts.

14. Joseph A. Schwartz, (Ph. D. Thesis), Lawrence Radiation Laboratory report UCRL-11360 June 1964 (unpublished).

15. A. Diddens, E. Jenkins, T. Kycia, and K. F. Riley, Phys. Rev. Letters 10, 262 (1963).

16. A. Citron, W. Galbraith, T. F. Kycia, B. A. Leontic, R. H. Phillips, and A. Rousset, Phys. Rev. Letters 13, 205 (1964). See also Phys. Rev. 144, 1101 (1966).

17. D. R. O. Morrison, review paper delivered at the Conference on Two-Body Reactions, Stony Brook, April 1966 (to be published).

18. The following guideline was used for selecting the highest-order polynomial used for fitting the angular distributions: Once the need for a certain order is indicated by a rise of the confidence level in the fit, at least that order is used for all higher beam momenta.

19. The break in the roughly exponential distribution near $t = -0.5$ $(BeV/c)^2$ and the secondary peak at larger values of $|t|$ in the $\Sigma^0 K^0$ channel is a common feature of many two-body reactions. The dip near $t = -0.5$ $(BeV/c)^2$ in the reaction $\pi^- p \rightarrow \pi^0 n$ has been interpreted as due to the vanishing of the helicity-flip amplitude at the zero in the ρ Regge trajectory by Arbab and Chiu [F. Arbab and C. B. Chiu, Phys. Rev. 147, 1045 (1966)]. Their idea has been generalized to other reactions by Frautschi [S. Frautschi, Phys. Rev. Letters 17, 722 (1966)].

20. The expression for the expansion coefficients can be written in a relatively simple form. The calculation is tedious to perform by hand however. We are grateful to Dr. Gerald Lynch for illuminating conversations on this point, and for the use of a computer program he has written to perform the expansion.

21. For a review of the analysis of other reactions in terms of baryon exchange, see Peter E. Schlein, Baryon Exchange and Production of $J \geq 3/2$ Baryons, in Lectures in Theoretical Physics (University of Colorado, Boulder, Colorado, 1966), Vol. VIIIB, p. 111 and L. Lyons Nuovo Cimento 43, A888 (1966).

22. The contribution of $I = 1$ baryon exchange to $\Sigma^0 K^0$ would have to be twice as large as to $\Sigma^- K^+$.

23. The relative size of the baryon exchange peaks in the three reactions considered can be understood in the framework of SU_3 invariance. If we assume that the $I = 0$ contribution comes from Λ, and that the $I = 1$ contribution comes from Σ and $Y_1^*(1385)$ exchange, the amplitudes for the three reactions become

$$A_{\Sigma^- K^+} = C_1 \Sigma + C_2 Y_1^*(1385) + C_3 \Lambda,$$
$$A_{\Sigma^0 K^0} = -\sqrt{2}\, C_1 \Sigma - \sqrt{2}\, C_2 Y_1^*(1385),$$
$$A_{\Lambda K^0} = C_4 \Sigma - \sqrt{6}\, C_2 Y_1^*(1385),$$

where the particle symbols on the right represent the contribution from the exchange of that object. If the ratio of d- and f-type coupling is $d/f > 1.0$, we find

(a) $C_3/C_1 \geq 3$,

(b) the relative sign of the coefficients for Σ and $Y_1^*(1385)$ is different for $\pi^- p \to \Lambda K^0$ and for $\pi^- p \to \Sigma K$.

For $d/f = 1.5$, for example, we have

$$C_1 = 4/25, \quad C_2 = 1/6, \quad C_3 = 18/25, \text{ and } \quad C_4 = 2\sqrt{6}/25.$$

The lack of a baryon exchange peak in the $\pi^- p \to \Sigma^0 K^0$ differential cross section can then be interpreted as destructive interference between the Σ and the $Y_1^*(1385)$. The same holds for $\pi^- p \to \Sigma^- K^+$, and Λ exchange is expected to give a large cross section. For the reaction $\pi^- p \to \Lambda K^0$ the interference between Σ and $Y_1^*(1385)$ becomes constructive, and a sizeable baryon exchange peak can be expected, as is found in the experiment.

We thank Professor David Jackson for bringing this argument to our attention.

24. Data on the reaction $\pi^+ p \to \Sigma^+ K^+$, and a comparison with the other ΣK channels along the lines outlined here have recently been presented. See R. R. Kofler, R. H. Hartung, and D. D. Reeder, The Reaction $\pi^+ p \to \Sigma^+ K^+$ at 3.23 GeV/c, Contribution to the XIIIth International Conference on High Energy Physics, August 31–September 7, 1966 Berkeley, California (proceedings to be published by the University of California Press, Berkeley).

25. Actually the terms in the sum were weighted by the inverse of the detection probability ϵ_i. The complete sum, including the error is then

$$\sum_i \frac{\cos \xi_i}{\epsilon_i} \pm \sqrt{\sum_i \left(\frac{\cos \xi_i}{\epsilon_i}\right)^2} .$$

See F. T. Solmitz, Ann. Rev. Nucl. Sci. 14, 375 (1964), especially p. 399.

26. Our results are in good agreement with the polarization measurements

at 1.5 BeV/c by Yoder et al.,[2] at 1.59 BeV/c by Goussu et al.,[3] and at 1.5 and 1.8 BeV/c by Kim et al.[1]

27. K. V. L. Sarma and D. D. Reeder, A Regge Pole Analysis of the Reaction $\pi^+ p \rightarrow \Sigma^+ K^+$ at 3.23 GeV/c, University of Wisconsin preprint, August 1966.

28. A model involving two Regge-pole exchange has also been developed by Arnold (R. C. Arnold, Double Octet Regge-Pole Model with Exchange Degeneracy for Charge- and Hypercharge-Exchange Reactions, to be published in Phys. Rev.).

29. Polarization of the Σ^0 has been measured at 1.5 and 1.8 BeV/c by Y. S. Kim, G. R. Burleson, P. I. P. Kalmus, A. Roberts, and T. A. Romanowsky, Phys. Rev. 143, 1028 (1966).

30. For a list of references on this subject see S. Frautschi, Ref. 19.

Table I. Cross section for associated production.

p_{beam}[a] (BeV/c)	$E_{c.m.}$ (BeV)	$\pi^- p \to \Lambda K^0$		$\pi^- p \to \Sigma^0 K^0$		$\pi^- p \to \Sigma^- K^+$		Reference	Symbol on Fig. 1
		σ (μb)	Events	σ (μb)	Events	σ (μb)	Events		
1.50	1.930	334±19	308	167±22	59	242±14	293	14	▽
1.508	1.934	214±23	476	~177	134			2	◇
1.59	1.974	214±21	106[b]	178±22	65	262±16	285	3	▲
1.615	1.985	208±25	286	111±20	70	180±20	319	Pres. exp.	○
1.69	2.020	199±12	263	110±14	58	153± 9	266	14	▽
1.85	2.093	181±12	215	140±17	66	99± 8	153	14	▽
1.94	2.133	185±15	436	126±15	127	98±10	281	Pres. exp.	○
1.95	2.137	182±11	255	94±13	53	99± 7	182	14	▽
1.98	2.150	184±20	299	116±15	87	90±10	191	Pres. exp.	○
2.05	2.181	182±17	119	123±21	33	70± 9	60	14	▽
2.05	2.181	179±15	515	113±10	153	87± 8	327	Pres. exp.	○
2.14	2.219	162±20	78	100±20	23	39±10	25	Pres. exp.	○
2.15	2.223	192±11	334	114±13	82	65± 5	148	14	▽
2.25	2.265	172±10	319	105±12	80	57± 5	138	14	▽
2.35	2.310	174±14	157	113±18	41	53± 7	63	14	▽
2.605	2.407	106±12	182	81±12	66	30± 5	67	Pres. exp.	○
2.70	2.444	120±11		85±12		31± 5		4	■
2.75	2.463	90±25	18	95±25	19	32±10	15	5	◆
2.86	2.505	109±15	59	93±25	26	22± 7	18	Pres. exp.	○
3.00	2.556	31±14	5	86±25	14	15± 5	12	6	●
3.01	2.560	84±12	111	74±12	52	22± 4	43	Pres. exp.	○
3.125	2.602	94±12	170	41±10	39	15.5±3.0	41	Pres. exp.	○
3.21	2.632	87±10	301	50± 6	91	15.5±2.0	76	Pres. exp.	○
2.885	2.862	67±12	86	37± 8	22	8.5±2.5	16	Pres. exp.	○
4.00	2.900	c		c		5.0±3.0	2	7	△
4.16	2.948	49± 8	75	42± 8	30	4.5±1.5	10	Pres. exp.	○
4.65	3.103	d		d			0	8	

a. The momentum bite is typically between ±0.03 and ±0.05 BeV/c.

b. This value does not include events where only a $\Lambda \to p\pi^-$ decay is seen.

c. $\sigma_{\pi^- p \to \Lambda K^0} + \sigma_{\pi^- p \to \Sigma^0 K^0}$ = 93±14 μb based on 39 events is given in Ref. 7.

d. $\sigma_{\pi^- p \to \Lambda K^0} + \sigma_{\pi^- p \to \Sigma^0 K^0}$ = 40 μb based on 8 events is reported in Ref. 8.

Table II. Differential cross section in units of μb/sr as a function of the beam momentum and the production angle.

(a) $\pi^- p \rightarrow \Lambda K^0$

P_{beam} (BeV/c)	Cos θ												
	-1.0	-0.9	-0.8	-0.6	-0.4	-0.2	0.0	0.2	0.4	0.6	0.8	0.9	0.95	1.0
1.50	41.6±9.6	25.8±7.2	8.6±2.9	4.7±2.1	4.6±2.1	5.5±2.3	20.6±4.4	28.8±5.2	37.9±6.0	37.7±6.0	76.0±12.2	110.2±20.8	76.6±17.6	
1.60	38.5±6.6	23.0±5.1	6.5±1.8	1.1±0.8	5.0±1.6	11.3±2.4	9.9±2.2	14.2±2.7	13.8±2.6	20.9±3.2	40.8±6.5	56.4±10.9	71.3±12.4	
1.70	41.9±7.8	28.4±6.2	6.5±2.0	1.3±0.9	2.5±1.3	5.8±1.9	8.2±2.3	9.5±2.5	16.5±3.2	24.7±4.0	30.4±6.3	65.5±13.4	66.8±13.6	
1.86	19.2±5.0	17.1±4.6	8.9±2.3	1.8±1.0	4.1±1.5	4.7±1.7	6.9±2.0	6.3±1.9	13.8±2.8	21.3±3.6	34.8±6.5	73.7±13.5	86.5±14.8	
1.95	29.0±3.2	15.9±2.3	7.8±1.1	3.0±0.7	1.7±0.5	2.1±0.6	3.8±0.8	9.4±1.2	11.8±1.4	18.6±1.7	37.5±3.5	68.2±6.8	118.4±9.1	
2.05	23.1±3.2	14.4±2.5	6.8±1.2	1.9±0.6	2.1±0.7	2.5±0.7	5.2±1.0	10.4±1.5	14.0±1.7	19.0±2.0	30.4±3.6	70.3±7.9	122.9±10.6	
2.20	12.8±2.5	11.3±2.3	5.2±1.1	2.5±0.8	1.3±0.5	2.1±0.7	1.7±0.6	6.1±1.2	11.9±1.6	19.1±2.0	38.1±4.1	91.6±9.1	144.6±11.7	
2.35	12.4±5.1	5.9±3.4	3.1±1.8	2.9±1.7	1.0±1.0	2.9±1.7	3.2±1.9	7.7±2.7	8.6±2.9	18.6±4.3	37.4±8.6	84.6±18.5	168.5±26.6	
2.60	6.7±2.5	0.0±0.9	1.4±0.8	0.0±0.5	0.9±0.7	0.9±0.6	0.0±0.5	4.4±1.4	8.7±2.0	11.2±2.2	29.5±5.2	50.5±9.7	106.4±14.5	
3.15	3.5±0.9	1.2±0.5	0.0±0.1	0.3±0.2	0.8±0.3	1.3±0.4	0.9±0.3	2.1±0.5	5.0±0.8	8.1±1.0	14.3±1.8	49.7±4.9	119.0±7.8	
4.00	3.1±1.4	1.2±0.9	0.3±0.3	0.0±0.3	0.0±0.3	0.0±0.3	0.0±0.3	0.4±0.4	0.0±0.3	3.6±1.1	10.1±2.5	22.7±5.2	123.0±12.3	

(b) $\pi^- p \rightarrow \Sigma^0 K^0$

P_{beam} (BeV/c)	Cos θ											
	-1.0	-0.8	-0.6	-0.4	-0.2	0.0	0.2	0.4	0.6	0.8	0.9	0.95	1.0
1.50	9.1±5.2	15.5±7.1	42.1±11.5	4.8±3.4	6.9±4.0	3.3±3.3	4.5±3.2	12.2±5.5	9.0±4.5	9.1±6.5	30.9±18.1	52.8±23.9	
1.60	1.5±1.5	9.2±3.5	14.0±4.2	6.2±2.8	4.8±2.4	5.9±2.7	9.4±3.3	1.2±1.2	4.8±2.4	12.0±5.4	57.0±17.4	44.2±14.7	
1.70	0.0±1.1	11.1±4.0	10.1±3.9	4.6±2.3	3.9±2.3	5.5±2.5	4.4±2.2	7.2±3.0	3.3±1.9	36.4±9.5	38.1±13.5	40.1±14.3	
1.86	3.9±2.8	9.1±3.8	7.6±3.1	3.7±2.1	1.2±1.2	3.7±2.1	12.8±4.1	14.4±4.4	7.2±2.9	9.7±4.9	62.9±20.1	77.1±20.8	
1.95	5.5±1.7	3.2±1.1	6.5±1.6	6.7±1.6	7.2±1.7	11.5±2.2	9.3±1.9	7.1±1.7	5.5±1.5	21.0±4.0	47.1±8.5	36.8±7.5	
2.05	2.3±1.1	3.3±1.2	4.2±1.4	7.0±1.8	5.8±1.6	8.3±1.9	13.6±2.5	7.7±1.8	5.5±1.5	16.0±3.8	34.0±7.8	53.1±9.9	
2.20	2.0±1.2	1.7±1.0	1.9±0.9	5.0±1.6	6.3±1.8	10.1±2.4	14.7±2.7	9.3±2.2	7.6±2.0	14.6±4.0	31.6±8.0	43.0±9.5	
2.35	0.0±2.4	0.0±2.4	2.4±2.4	0.0±2.4	19.0±7.4	4.6±3.2	9.0±4.5	8.4±5.0	15.8±6.6	18.7±9.4	23.7±16.8	63.8±26.4	
2.60	0.0±1.0	1.0±1.0	1.0±1.0	0.0±1.0	2.0±1.4	7.7±2.7	5.0±2.2	9.4±3.0	4.7±2.1	11.4±4.7	27.6±10.4	84.2±18.4	
3.15	0.3±0.3	0.3±0.3	0.0±0.3	0.3±0.3	0.7±0.4	2.0±0.7	3.2±0.9	5.6±1.2	5.4±1.2	7.4±1.9	13.2±3.6	82.0±9.3	
4.00	0.0±0.6	0.0±0.6	0.0±0.6	0.0±0.6	0.0±0.6	0.0±0.6	0.0±0.6	0.6±0.6	4.2±1.6	7.7±3.2	19.0±6.7	70.5±13.7	

(c) $\pi^- p \rightarrow \Sigma^- K^+$

P_{beam} (BeV/c)	Cos θ									
	-1.0	-0.8	-0.6	-0.4	-0.2	0.0	0.2	0.4	0.6	0.8	1.0
1.50	62.0±6.8	40.5±5.6	27.1±4.5	16.0±3.5	16.9±3.6	12.4±3.1	5.5±2.1	4.8±2.0	0.8±0.8	7.0±2.5	
1.60	36.5±3.9	36.0±3.8	24.1±3.2	17.0±2.7	13.4±2.4	6.3±1.6	4.8±1.4	3.1±1.2	0.4±0.4	1.4±0.8	
1.70	23.7±3.2	23.4±3.2	18.7±2.9	15.6±2.6	15.2±2.7	9.9±2.1	8.7±2.0	2.9±1.2	1.5±0.9	2.0±1.0	
1.86	14.3±2.6	10.8±2.3	14.7±2.6	6.2±1.7	7.7±1.9	9.2±2.1	8.9±2.1	3.7±1.4	2.1±1.0	1.7±1.0	
1.95	15.8±1.4	14.3±1.3	11.2±1.2	10.0±1.1	6.6±0.9	6.7±0.9	5.3±0.8	4.6±0.8	1.2±0.4	0.9±0.4	
2.05	12.3±1.4	12.2±1.4	9.7±1.2	8.9±1.2	6.9±1.1	4.7±0.9	3.8±0.8	2.7±0.7	1.5±0.5	0.6±0.3	
2.20	16.4±1.6	7.2±1.1	7.9±1.1	4.4±0.8	3.0±0.7	2.3±0.6	3.5±0.8	1.0±0.4	0.2±0.2	0.8±0.4	
2.35	17.0±3.6	8.5±2.6	3.1±1.6	4.0±1.8	1.6±1.2	0.8±0.8	2.4±1.4	1.7±1.2	0.8±0.8	1.8±1.2	
2.60	9.1±1.8	6.3±1.5	3.8±1.2	1.4±0.7	1.1±0.6	0.8±0.6	0.4±0.4	0.0±0.4	0.4±0.4	0.0±0.4	
3.15	6.2±0.7	3.4±0.5	1.8±0.4	1.0±0.3	0.3±0.2	0.5±0.2	0.0±0.1	0.1±0.1	0.0±0.1	0.6±0.3	
4.00	2.6±0.7	1.0±0.4	0.6±0.3	0.0±0.2	0.0±0.2	0.2±0.2	0.0±0.2	0.0±0.2	0.2±0.2	0.2±0.2	

Table III. Coefficients of the least-squares fit of Legendre polynomials to the angular distribution:

$$\frac{d\sigma}{d\Omega} = \sum_n A_n P_n (\cos\theta)$$

(a) $\pi^- p \rightarrow \Lambda K^0$

P_{beam} (BeV/c)	Coefficients											
	A_0	A_1	A_2	A_3	A_4	A_5	A_6	A_7	A_8	A_9	A_{10}	A_{11}
1.50	25.4±1.6	25.8±3.4	33.7±4.5	-6.1±4.7	9.6±4.8							
1.60	16.4±1.0	11.4±2.0	26.1±2.7	-0.6±2.7	21.7±3.0							
1.70	15.4±1.0	10.4±2.3	28.1±3.1	-2.7±2.8	16.5±3.2							
1.86	13.9±1.0	15.3±2.1	26.9±2.8	10.0±3.3	15.1±3.1	5.7±3.4						
1.95	14.5±0.5	16.2±1.2	33.7±1.6	13.1±1.9	22.8±2.1	14.2±2.3	12.4±2.0	5.5±2.1				
2.05	14.3±0.5	17.7±1.3	31.0±1.8	13.4±2.2	23.4±2.5	18.2±2.7	17.0±3.0	11.0±2.5	4.7±2.8			
2.20	13.9±0.6	23.3±1.4	36.0±1.9	25.2±2.3	25.9±2.6	22.0±2.7	18.3±3.1	13.2±2.4	6.3±2.6			
2.35	13.6±1.2	24.7±2.9	35.7±4.1	27.8±4.9	31.0±5.6	22.5±5.8	20.6±6.3	9.0±5.2	7.8±5.1			
2.60	8.3±0.6	18.1±1.6	23.4±2.2	18.5±2.6	19.3±2.9	15.4±3.1	18.0±3.3	11.4±2.6	7.8±2.4			
3.15	7.0±0.3	15.9±0.8	21.6±1.1	21.1±1.4	23.2±1.6	20.3±1.7	21.0±1.8	17.4±1.8	12.5±1.7	6.7±1.4	3.0±1.4	
4.00	4.4±0.4	11.0±1.1	17.8±1.7	18.8±2.1	20.9±2.5	19.7±2.8	18.5±2.8	17.4±3.0	14.2±2.7	13.2±2.7	7.3±1.6	6.0±1.9

(b) $\pi^- p \rightarrow \Sigma^0 K^0$

P_{beam} (BeV/c)	A_0	A_1	A_2	A_3	A_4	A_5	A_6	A_7	A_8	A_9	A_{10}
1.50	10.4±1.7	0.4±3.4	9.5±4.2	11.9±5.8	-3.1±7.5	10.2±7.0	8.8±8.6				
1.60	7.9±1.0	4.8±2.0	7.9±2.7	17.4±3.3	7.0±4.1	12.7±4.3	2.8±4.8				
1.70	7.9±1.0	6.5±2.1	8.9±2.8	17.0±3.5	4.3±4.1	14.5±4.1	2.9±5.2				
1.86	9.5±1.1	9.3±2.4	10.7±3.1	9.6±4.0	8.5±5.0	16.1±4.6	18.4±5.7				
1.95	8.9±0.6	7.5±1.2	6.8±1.7	9.7±1.9	14.6±2.0	8.0±2.2	5.0±2.8				
2.05	8.4±0.6	9.1±1.2	6.7±1.8	10.6±1.9	14.7±2.1	12.5±2.4	8.4±2.9				
2.20	8.4±0.7	10.0±1.3	4.2±1.8	4.7±2.0	11.5±2.4	9.9±2.6	4.7±2.8				
2.35	7.3±1.5	12.8±3.1	8.5±4.2	6.3±5.0	6.7±6.0	5.5±6.0	3.4±7.2				
2.60	5.8±0.8	11.0±1.7	9.5±2.5	9.7±3.1	11.5±3.1	15.2±3.8	8.9±3.5	5.0±4.4			
3.15	4.2±0.3	9.2±0.8	9.8±1.2	9.5±1.5	11.5±1.7	13.1±1.8	13.4±1.9	11.7±2.0	10.0±2.1	6.1±1.8	3.5±1.5
4.00	3.0±0.5	8.2±1.2	11.4±1.8	12.3±2.2	12.1±2.6	10.9±2.8	10.6±3.1	9.3±3.0	8.6±3.1	5.6±2.4	4.1±2.3

(c) $\pi^- p \rightarrow \Sigma^- K^+$

P_{beam} (BeV/c)	A_0	A_1	A_2	A_3	A_4
1.5	18.3±1.2	-28.2±2.2	14.1±2.5		
1.6	14.0±0.8	-22.0±1.4	9.1±1.4		
1.7	11.8±0.7	-14.3±1.3	2.6±1.4		
1.86	7.4±0.6	-6.5±1.0	-0.2±1.3		
1.95	7.5±0.3	-8.4±0.6	1.0±0.6		
2.05	6.3±0.3	-7.1±0.6	0.8±0.6		
2.20	4.3±0.3	-6.8±0.5	3.2±0.7	-0.6±0.6	
2.35	3.8±0.5	-5.9±1.2	5.5±1.4	-3.0±1.5	
2.60	2.3±0.3	-4.4±0.6	3.2±0.7	-1.3±0.6	
3.15	1.3±0.1	-2.6±0.3	2.6±0.3	-1.1±0.3	0.6±0.3
4.0	0.5±0.1	-0.9±0.2	1.2±0.3	-0.7±0.3	0.3±0.4

Table IV. Least-squares fit of the energy dependence of the cross sections to the expression $\frac{d\sigma}{dt}$ (or $\frac{d\sigma}{du}$) = $F(E_{c.m.})^m$.

Reaction	Momentum transfer interval $(BeV/c)^2$	Data points	χ^2	m
$\pi^- p \rightarrow \Lambda K^0$	$0 < t_0 - t < 0.4$	10[a]	15.8	- 2.0±0.4
	$0.4 < t_0 - t < 0.8$	10[a]	8.5	- 4.7±0.5
	$0 < u_0 - u < 1.0$	10[a]	18.3	-10.5±0.6
$\pi^- p \rightarrow \Sigma^0 K^0$	$0 < t_0 - t < 0.4$	11	3.0	- 1.5±0.6
	$0.4 < t_0 - t < 0.8$	11	10.1	- 5.1±0.8
$\pi^- p \rightarrow \Sigma^- K^+$	$0 < u_0 - u < 1.0$	11	13.3	- 9.8±0.4
	$1.0 < u_0 - u < 2.0$	7[b]	3.8	-11.5±0.9

a. The point at 1.5 BeV/c was eliminated because it fell several standard deviations outside the fit.

b. Only data above 1.9 BeV/c were used, because at lower momentum, kinematics does not allow the momentum transfer $u_0 - u = 2(BeV/c)^2$.

Table V. Distribution of the polarization times the differential cross section for the reaction $\pi^- p \rightarrow \Lambda K^0$. The values of $aP(d\sigma/d\Omega)$ are given in units of μb/sr as a function of beam momentum and production angle.

	Cos θ										
p_{beam} (BeV/c)	-1.0	-0.8	-0.6	-0.4	-0.2	0.0	0.2	0.4	0.6	0.8	0.9	1.0
1.50	10.0±10.4	0.7±1.9	-3.1±3.5	-9.4±4.9	-3.6±2.7	-6.2±9.2	-7.0±10.2	23.6±11.7	16.9±10.8	64.2±18.2	70.4±25.6	
1.60	3.6±6.9	0.4±3.5	-0.1±1.2	1.3±2.1	-6.1±5.1	-5.1±3.9	1.6±6.2	9.5±4.9	12.9±5.7	8.4±13.1	7.0±16.0	
1.70	7.0±8.2	1.3±4.7	2.7±1.9	-4.1±2.9	-1.5±4.2	-7.1±5.0	-7.2±4.2	11.1±5.7	12.0±7.0	4.3±10.1	3.5±15.6	
1.86	5.3±6.9	-5.7±4.1	1.8±1.6	-6.6±3.5	-3.0±2.1	-3.5±4.4	-5.3±3.3	7.1±5.3	10.9±6.6	23.8±11.7	11.1±18.8	
1.95	0.2±3.6	-1.5±2.1	1.0±1.5	-1.2±0.9	0.0±0.7	-2.1±1.6	-4.4±2.3	-2.1±2.6	-0.6±3.2	21.2±6.4	17.3±10.8	
2.05	4.4±3.7	-0.2±2.2	0.1±1.3	-1.9±1.4	0.3±1.1	-1.9±1.8	0.2±2.3	-2.6±3.3	4.0±3.4	24.0±7.0	37.5±12.5	
2.20	5.3±3.4	0.5±1.7	-1.3±1.5	-1.7±1.1	-0.2±1.1	-1.2±0.9	-2.5±1.9	-10.4±2.9	-3.8±3.5	26.3±7.8	14.7±14.3	
2.35	-1.2±5.7	-5.9±5.3	-5.3±3.8	-3.5±3.5	1.2±3.6	3.9±4.4	-3.2±5.8	-9.3±5.9	-11.9±9.1	14.2±16.0	24.4±32.4	
2.60	3.6±2.0	1.7±1.3	-0.0±0.4	0.4±0.4	0.5±0.5	-0.0±0.4	-4.8±2.7	-5.4±3.0	-3.7±3.8	14.3±9.9	1.0±18.3	
3.15	1.6±0.8	-0.0±0.1	-0.1±0.1	1.0±0.8	-1.2±0.7	-0.3±0.7	0.0±0.7	-3.2±1.5	-4.8±1.7	7.2±3.6	10.8±8.7	
4.00	-1.1±2.0	0.3±0.3	-0.0±0.2	-0.0±0.2	-0.0±0.2	-0.0±0.2	1.2±1.2	-0.0±0.2	-1.9±2.0	-9.0±5.7	-6.3±12.3	

Table VI. Coefficients of the least-squares fit of the angular distribution of Λ polarization in the reaction $\pi^- p \to \Lambda K^0$ to the series

$$aP \frac{d\sigma}{d\Omega} = \sin\theta \sum_n B_n \frac{dP_{n+1}(\cos\theta)}{d(\cos\theta)}.$$

p_{beam} (BeV/c)	B_0	B_1	B_2	B_3	B_4	B_5	B_6
1.5	+5.0±2.8	+9.1±2.5	+10.8±2.2	+4.2±2.0	+3.6±1.7		
1.6	+2.4±1.7	+3.7±1.5	+3.1±1.5	+1.2±1.2	-0.3±1.1		
1.7	+5.0±1.8	+1.7±1.6	+3.9±1.6	+0.8±1.2	-0.9±1.1		
1.86	+1.1±1.6	+3.6±1.6	+4.2±1.5	+2.5±1.2	+0.2±1.0		
1.95	-0.2±0.8	+1.3±0.9	+2.3±0.8	+2.6±0.8	+1.9±0.7	+0.9±0.5	+0.3±0.5
2.05	+1.6±0.9	+2.3±0.9	+3.7±0.9	+2.6±0.8	+3.0±0.8	+1.3±0.6	+0.9±0.5
2.20	-1.1±0.8	-0.1±0.9	+2.8±0.9	+2.3±0.9	+3.4±0.8	+1.4±0.6	+0.8±0.5
2.35	-2.8±2.1	+0.8±2.2	-0.2±2.0	+2.1±1.9	+3.9±1.8	+2.1±1.5	+0.8±1.3
2.60	-0.4±0.8	-0.9±1.0	+1.4±1.0	+1.3±1.0	+2.0±0.9	+0.7±0.5	+0.3±0.4
3.15	-0.5±0.4	-0.3±0.4	+0.7±0.4	+0.7±0.4	+1.4±0.4	+0.9±0.3	+0.6±0.2
4.00	-0.7±0.4	-1.0±0.5	-1.1±0.6	-0.9±0.5	-0.7±0.4	-0.3±0.2	-0.2±0.2

FIGURE LEGENDS

Fig. 1. Total cross sections as a function of the total c.m. energy for the reactions $\pi^- p \to \Lambda K^0$, $\pi^- p \to \Sigma^0 K^0$, and $\pi^- p \to \Sigma^- K^+$. Log-log scale is used. The lines represent least-squares fits of the data to the expression $\sigma_T = A(E_{c.m.})^B$. The symbols are explained in Table I.

Fig. 2. Differential cross sections for the reaction $\pi^- p \to \Lambda K^0$. The angle θ is defined by $\cos\theta = \hat{P}_{K^0} \cdot \hat{P}_{beam}$ in the reaction c.m. The curves correspond to least-squares fits of Legendre polynomials to the data.

Fig. 3. Differential cross sections for the reaction $\pi^- p \to \Sigma^0 K^0$. The angle θ is defined by $\cos\theta = \hat{P}_{K^0} \cdot \hat{P}_{beam}$ in the reaction c.m. The curves correspond to least-squares fits of Legendre polynomials to the data.

Fig. 4. Differential cross sections for the reaction $\pi^- p \to \Sigma^- K^+$. The angle θ is defined by $\cos\theta = \hat{P}_{K^-} \cdot \hat{P}_{beam}$ in the reaction c.m. The curves correspond to least-squares fits of Legendre polynomials to the data.

Fig. 5. Momentum-transfer distribution in the region of peripheral peaking (a-c) for $\pi^- p \to \Lambda K^0$ and (d - f) for $\pi^- p \to \Sigma^0 K^0$. The lines represent maximum-likelihood fits to the expression $d\sigma/dt = C \exp[-D(t_0 - t)]$ in the region $0 < t_0 - t < 0.4$ (BeV/c)^2. The beam momenta and the fitted slope parameters are:

(a) 1.9-2.1 BeV/c; $D = 6.4 \pm 0.5$ (BeV/c)$^{-2}$
(b) 2.9-3.3 BeV/c; $D = 7.7 \pm 0.6$ (BeV/c)$^{-2}$
(c) 3.8-4.2 BeV/c; $D = 9.9 \pm 1.1$ (BeV/c)$^{-2}$

} for $\pi^- p \to \Lambda K^0$

(d) 1.9-2.1 BeV/c; $D = 7.5 \pm 1.0\ (\mathrm{BeV}/c)^{-2}$

(e) 2.9-3.3 BeV/c; $D = 10.7 \pm 1.2\ (\mathrm{BeV}/c)^{-2}$ } for $\pi^- p \to \Sigma^0 K^0$.

(f) 3.8-4.2 BeV/c; $D = 6.3 \pm 2.0\ (\mathrm{BeV}/c)^{-2}$

Fig. 6. Coefficients of the Legendre polynomial fit to the $\pi^- p \to \Lambda K^0$ angular distribution as a function of the beam momentum. The curves represent the expansion of the function $d\sigma/dt = C \exp[-7(t_0 - t)]$ in terms of Legendre polynomials.

Fig. 7. Momentum-transfer distribution in the u channel for $\pi^- p \to \Sigma^- K^+$. The lines represent maximum-likelihood fits to the expression $d\sigma/du = C \exp[-D(u_0 - u)]$ in the region $0 < u_0 - u < 1\,(\mathrm{BeV}/c)^2$. The beam momenta and the fitted slope parameters are (a) 1.9-2.1 BeV/c, $D = 0.79 \pm 0.12\ (\mathrm{BeV}/c)^{-2}$; (b) 2.9-3.3 BeV/c, $D = 1.30 \pm 0.30\ (\mathrm{BeV}/c)^{-2}$; (c) 3.8-4.2 BeV/c, $D = 1.45 \pm 0.8\ (\mathrm{BeV}/c)^{-2}$.

Fig. 8. Coefficients of the Legendre polynomial fit to the $\pi^- p \to \Sigma^- K^+$ angular distribution as a function of the beam momentum.

Fig. 9. Momentum-transfer distribution in the u channel for $\pi^- p \to \Lambda K^0$ at 1.9 to 2.1-BeV/c beam momentum. The line represents a maximum-likelihood fit to the expression $d\sigma/du = C \exp[-D(u_0 - u)]$ in the region $0 < u_0 - u < 0.5(\mathrm{BeV}/c)^2$. The fit yields $D = 4.2 \pm 0.6\ (\mathrm{BeV}/c)^{-2}$.

Fig. 10. Distribution of the quantity $\alpha_\Lambda P\,(d\sigma/d\Omega)$ for the reaction $\pi^- p \to \Lambda K^0$. The angle θ is defined by $\cos\theta = \hat{p}_{K^0} \cdot \hat{p}_{\mathrm{beam}}$ in the production c.m. The curves represent least-squares fits to the series $\sin\theta \sum_n B_n [dP_{n+1}(\cos\theta)]/d(\cos\theta)$.

Fig. 11. Polarization of the Λ in the reaction $\pi^- p \to \Lambda K^0$ as a function of the momentum transfer squared. The data for the 1.9 to 2.1-BeV/c interval are shown as circles; those for the 2.9 to 3.3-BeV/c interval are shown as triangles.

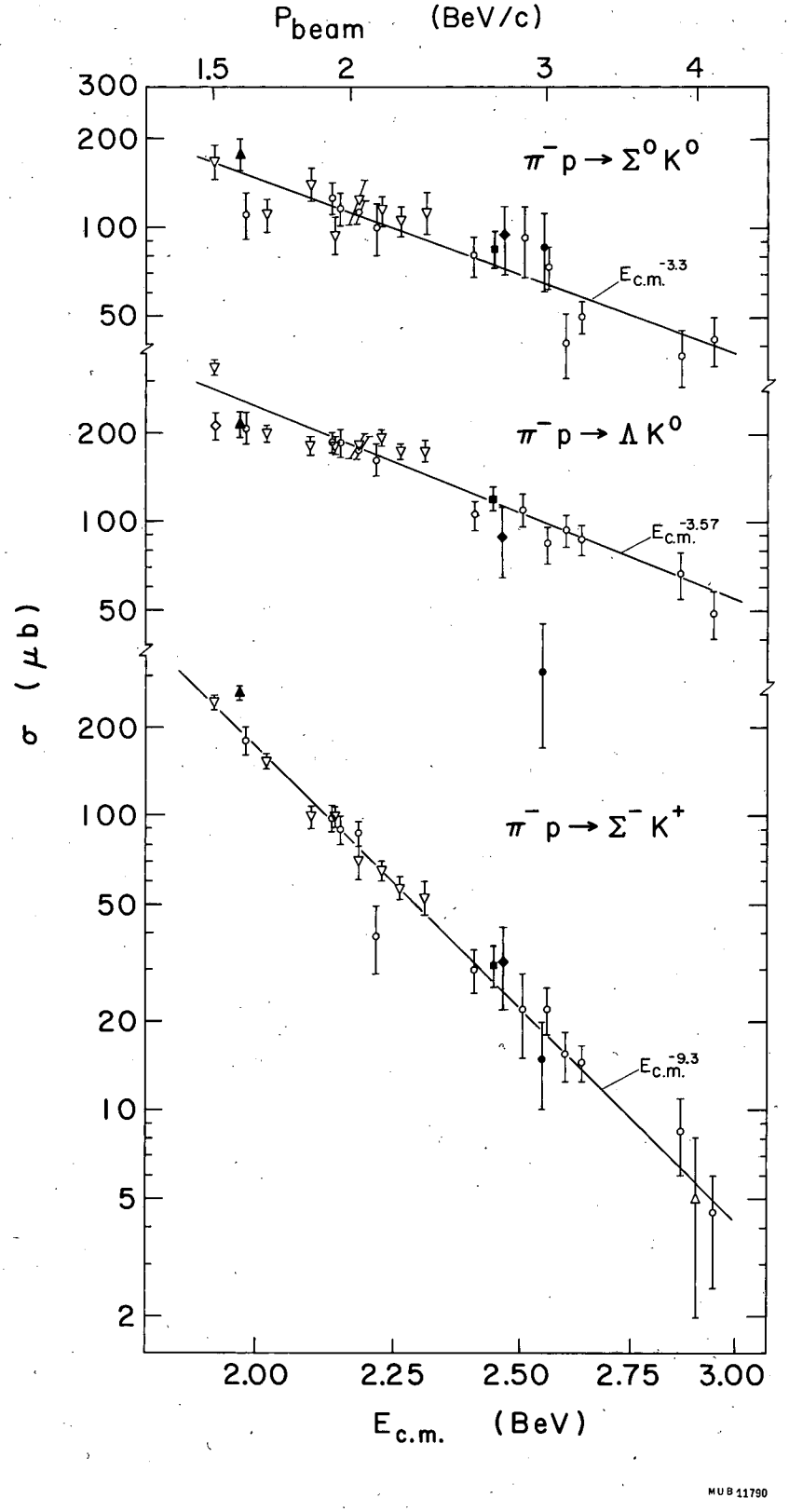
P beam (BeV/c)
1.5
2
3
4
300
200
100
50
200
100
50
200
100
50
20
10
5
2
σ (μb)
π⁻p → Σ⁰K⁰
E c.m. -3.3
π⁻p → ΛK⁰
E c.m. -3.57
π⁻p → Σ⁻K⁺
E c.m. -9.3
2.00
2.25
2.50
2.75
3.00
E c.m. (BeV)
MUB 11790

Fig. 1

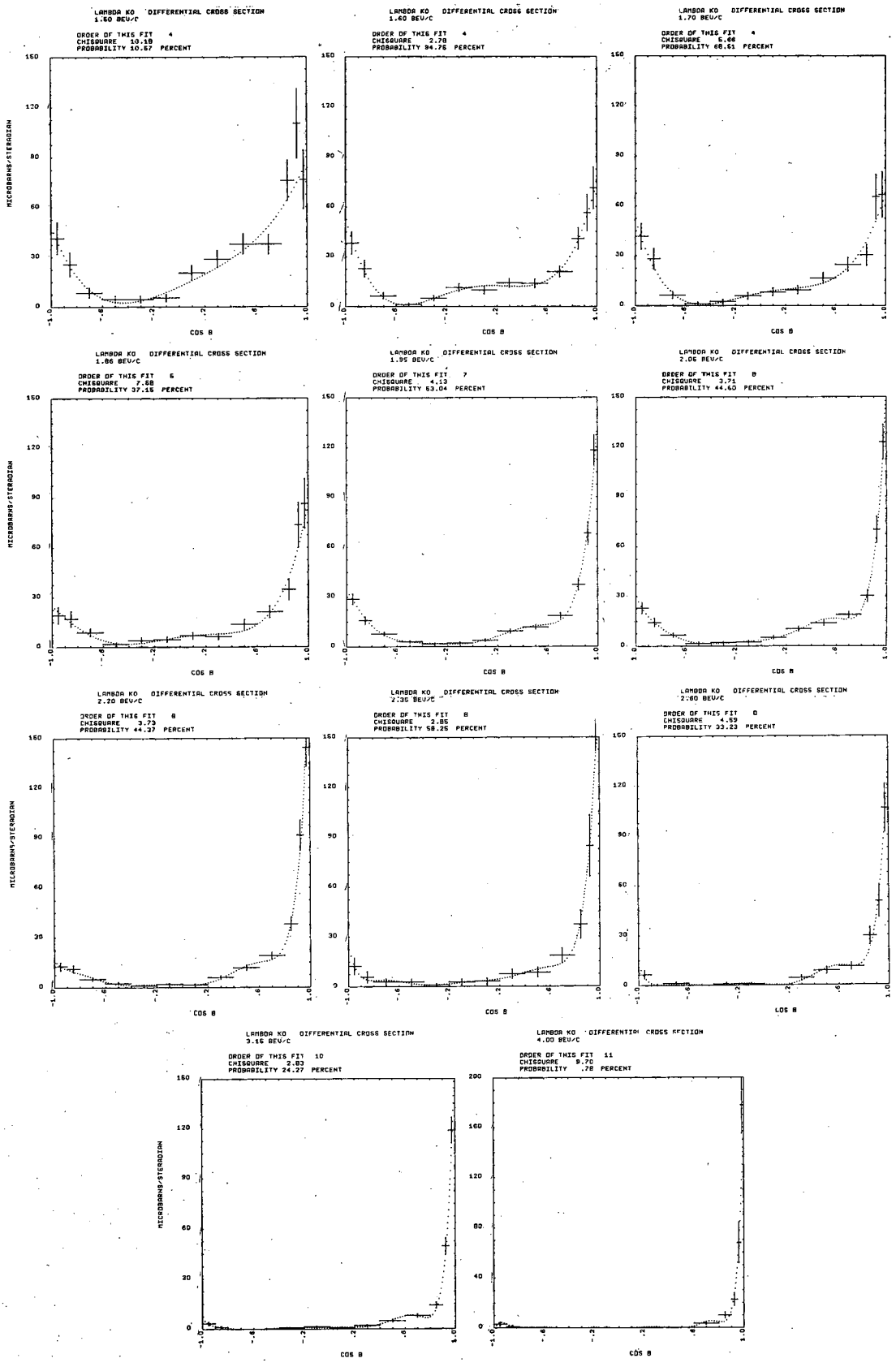

MUB 11637

Fig. 2

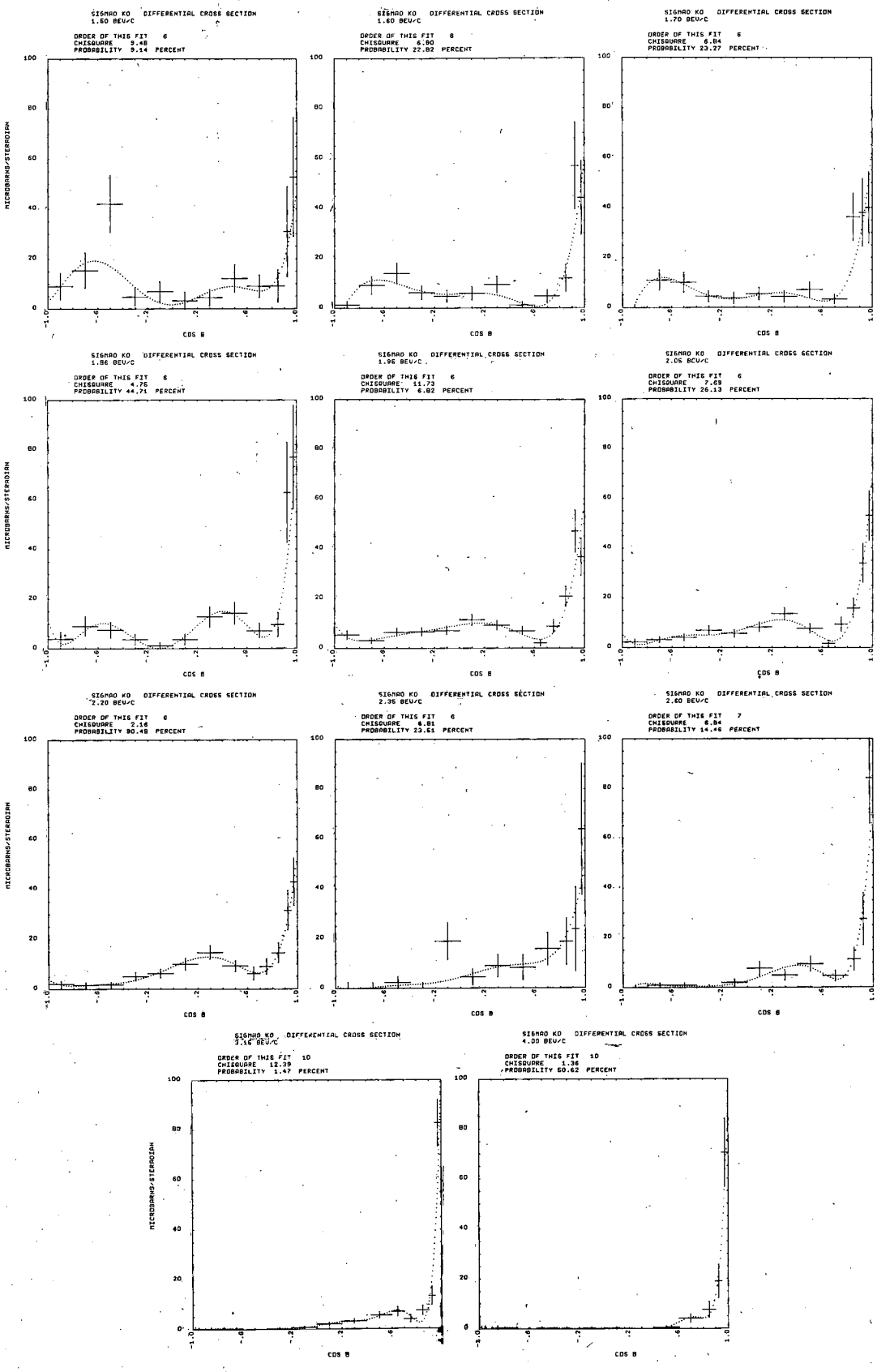

MUB-11635

Fig. 3

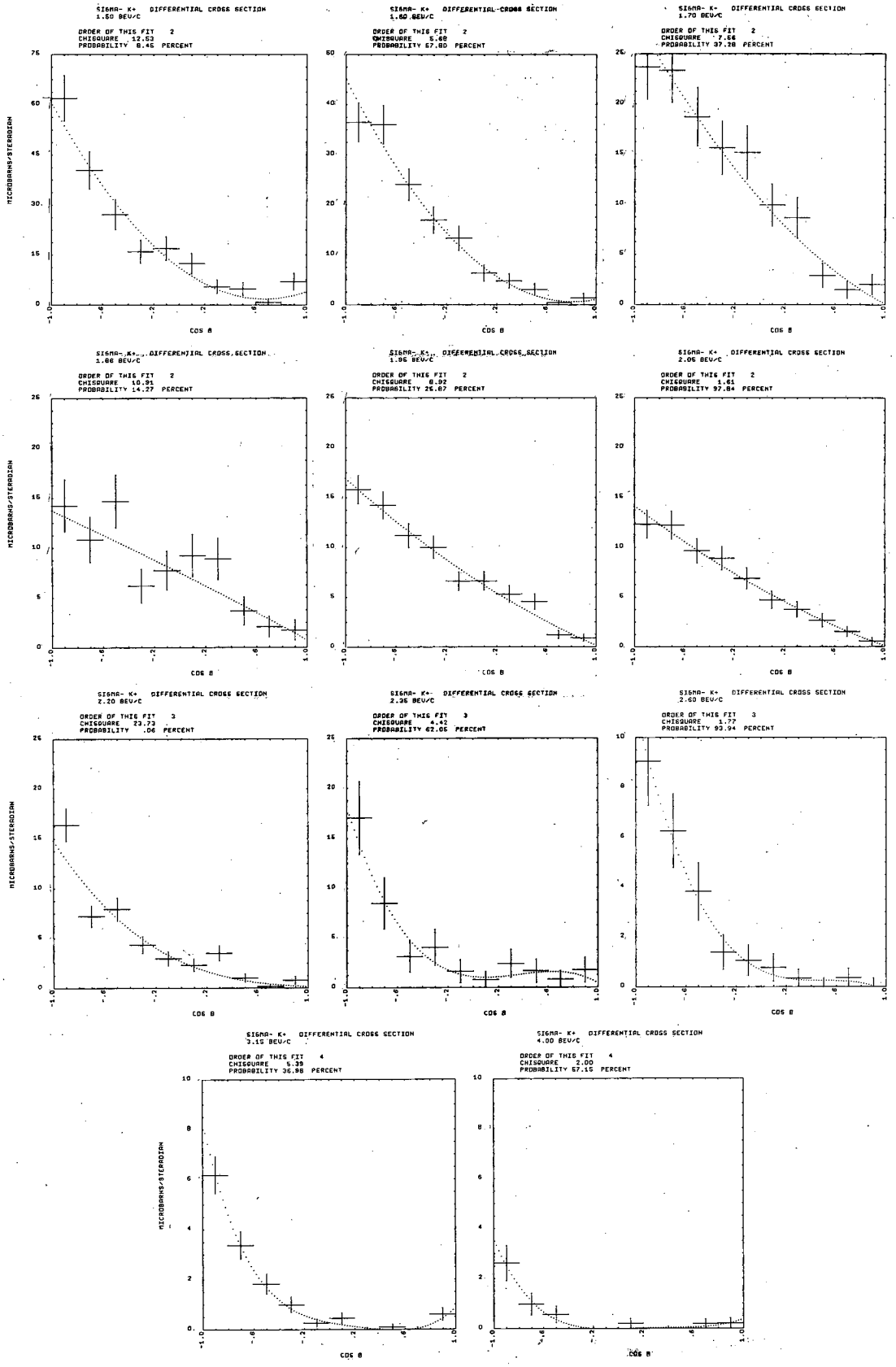

MUB-11634

Fig. 4

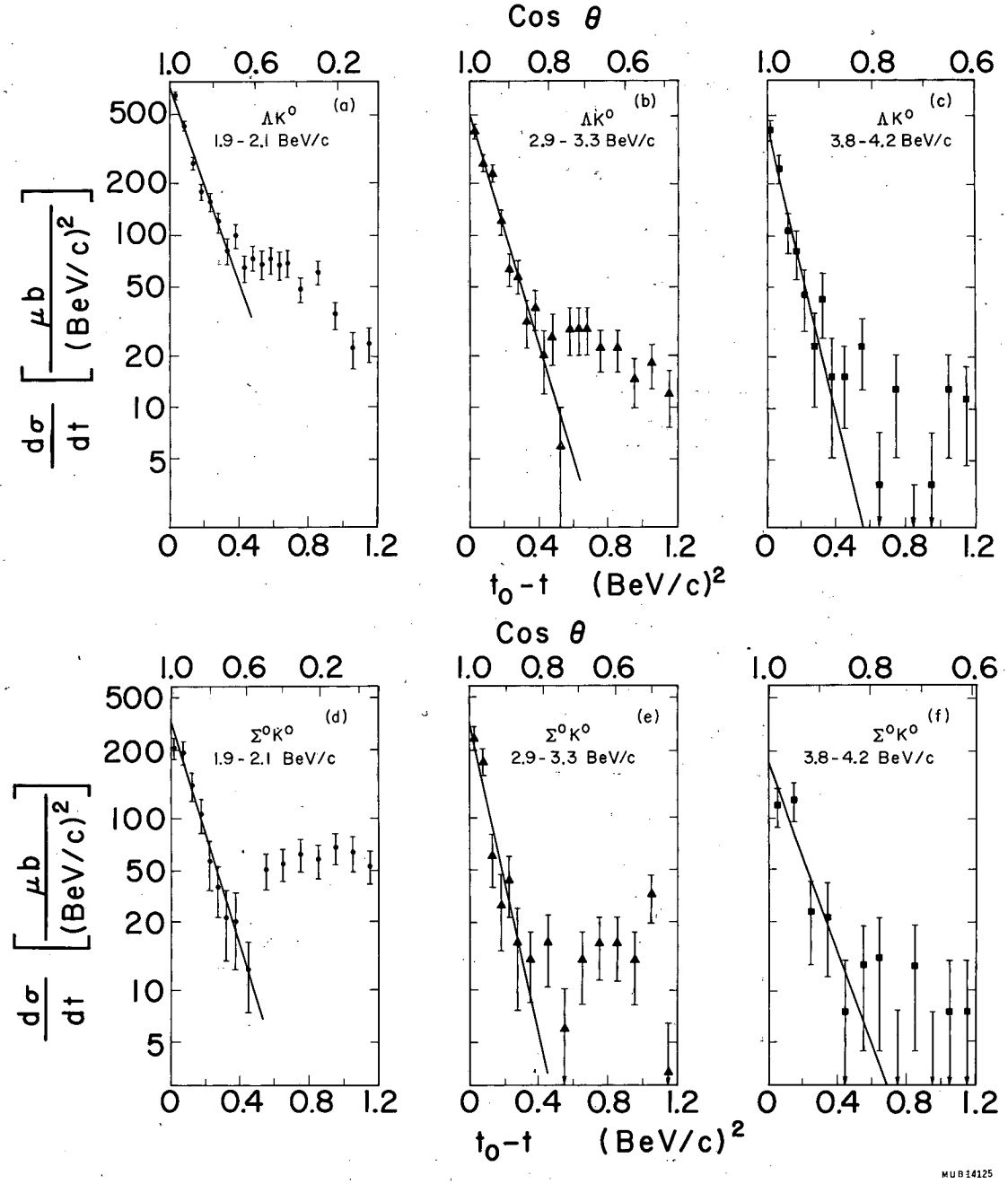
Cos θ
1.0 0.6 0.2
1.0 0.8 0.6
1.0 0.8 0.6
ΛK⁰ (a)
1.9 - 2.1 BeV/c
ΛK⁰ (b)
2.9 - 3.3 BeV/c
ΛK⁰ (c)
3.8 - 4.2 BeV/c
dσ/dt [μb/(BeV/c)²]
500
200
100
50
20
10
5
0 0.4 0.8 1.2
t₀ - t (BeV/c)²
Cos θ
Σ⁰K⁰ (d)
1.9 - 2.1 BeV/c
Σ⁰K⁰ (e)
2.9 - 3.3 BeV/c
Σ⁰K⁰ (f)
3.8 - 4.2 BeV/c
MUB 14125

Fig. 5

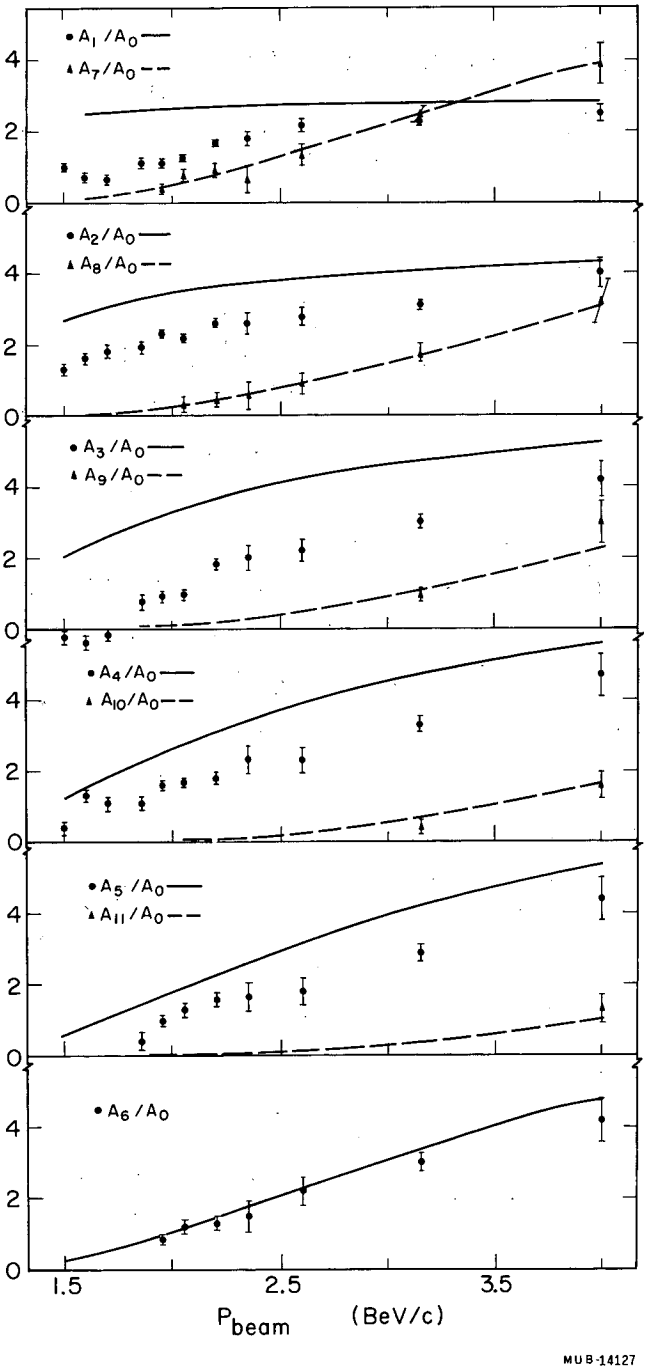
• A1 /A0 —
▲ A7/A0 - -
• A2/A0 —
▲ A8/A0 - -
• A3/A0 —
▲ A9/A0 - -
• A4/A0 —
▲ A10/A0 - -
• A5 /A0 —
▲ A11/A0 - -
• A6 /A0
0
2
4
1.5
2.5
3.5
Pbeam (BeV/c)
MUB-14127

Fig. 6

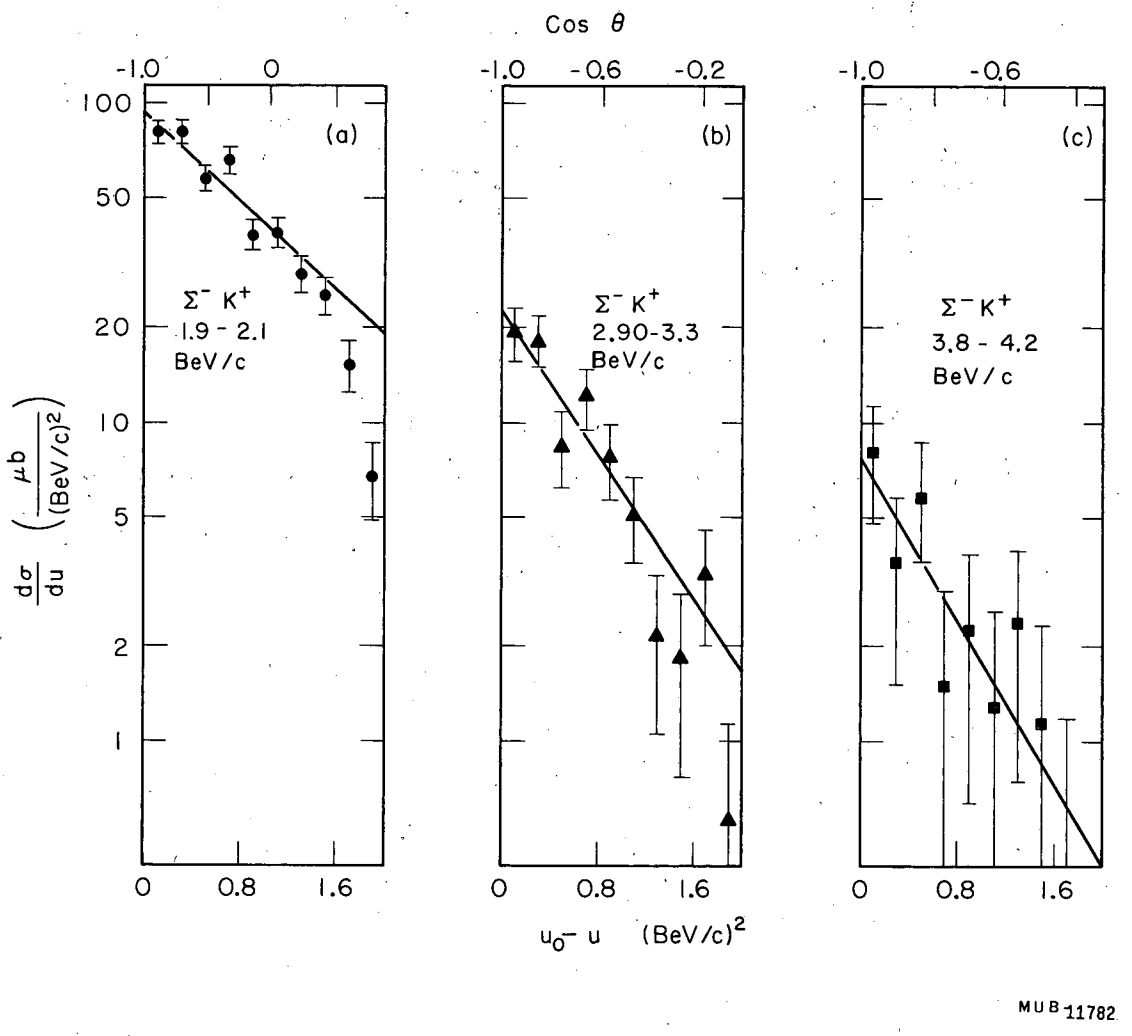
Cos θ
-1.0
0
-1.0
-0.6
-0.2
-1.0
-0.6
100
50
20
10
5
2
1
(a)
(b)
(c)
Σ⁻ K⁺
1.9 - 2.1
BeV/c
Σ⁻ K⁺
2.90-3.3
BeV/c
Σ⁻ K⁺
3.8 - 4.2
BeV/c
dσ/du (μb/(BeV/c)²)
0
0.8
1.6
0
0.8
1.6
0
0.8
1.6
u₀ − u (BeV/c)²
MUB 11782

Fig. 7

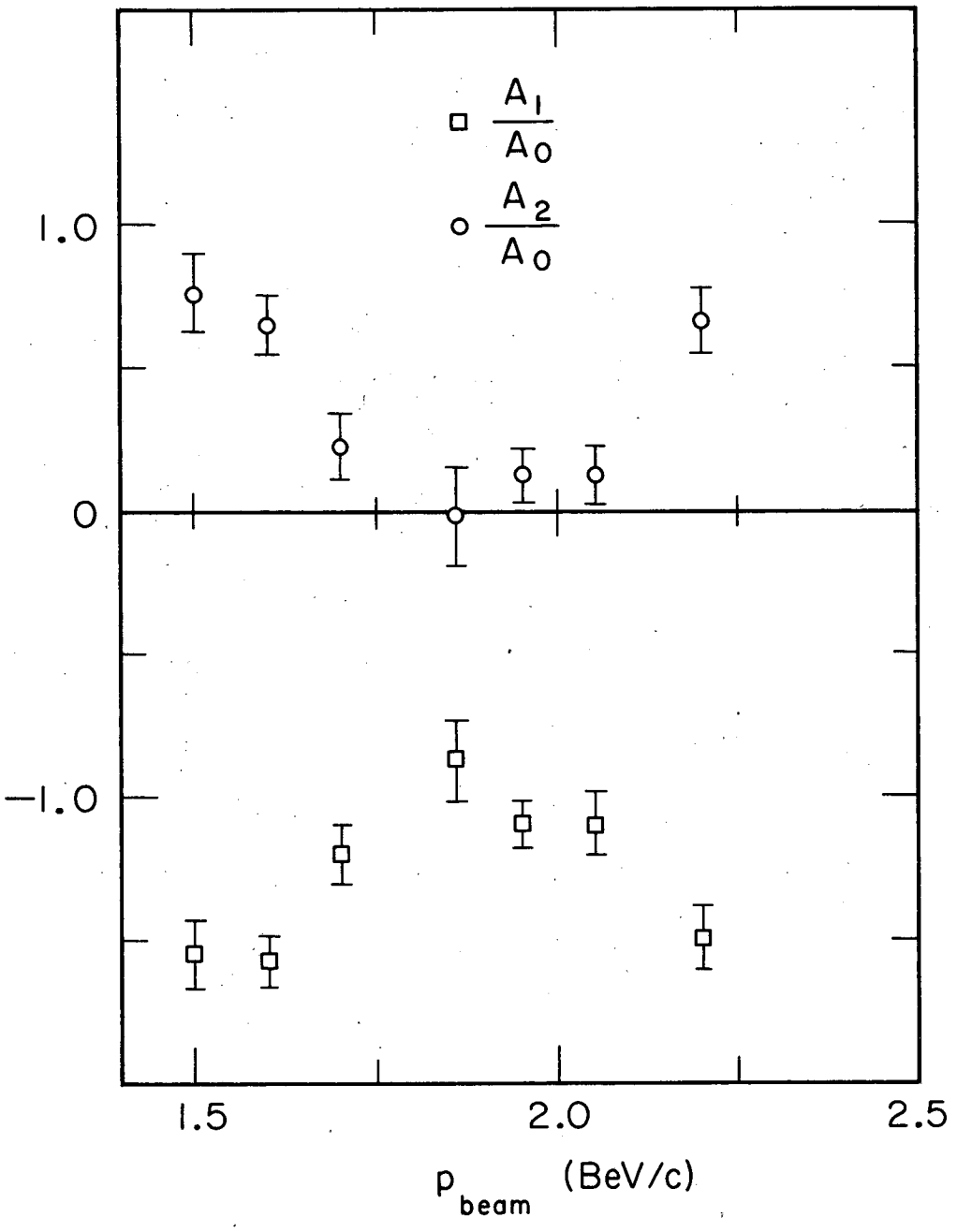

Fig. 8

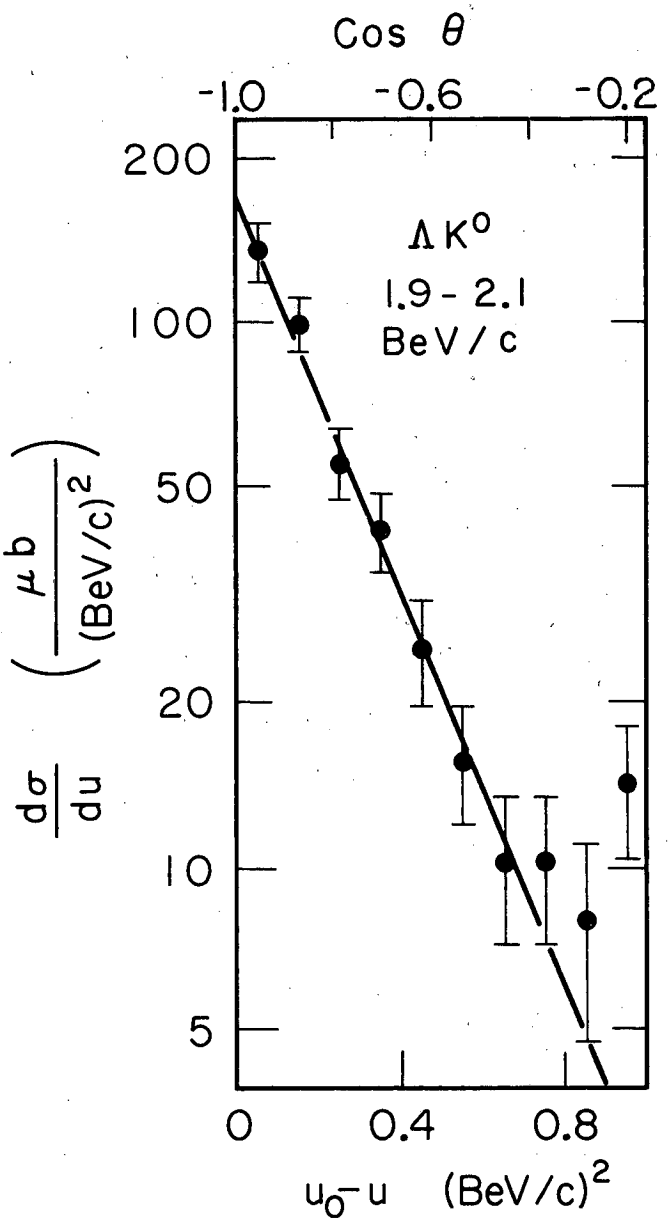
Cos θ
-1.0
-0.6
-0.2
200
100
50
20
10
5
ΛK⁰
1.9 - 2.1
BeV/c
dσ/du (μb/(BeV/c)²)
0
0.4
0.8
u₀-u (BeV/c)²
MUB-11784

Fig. 9

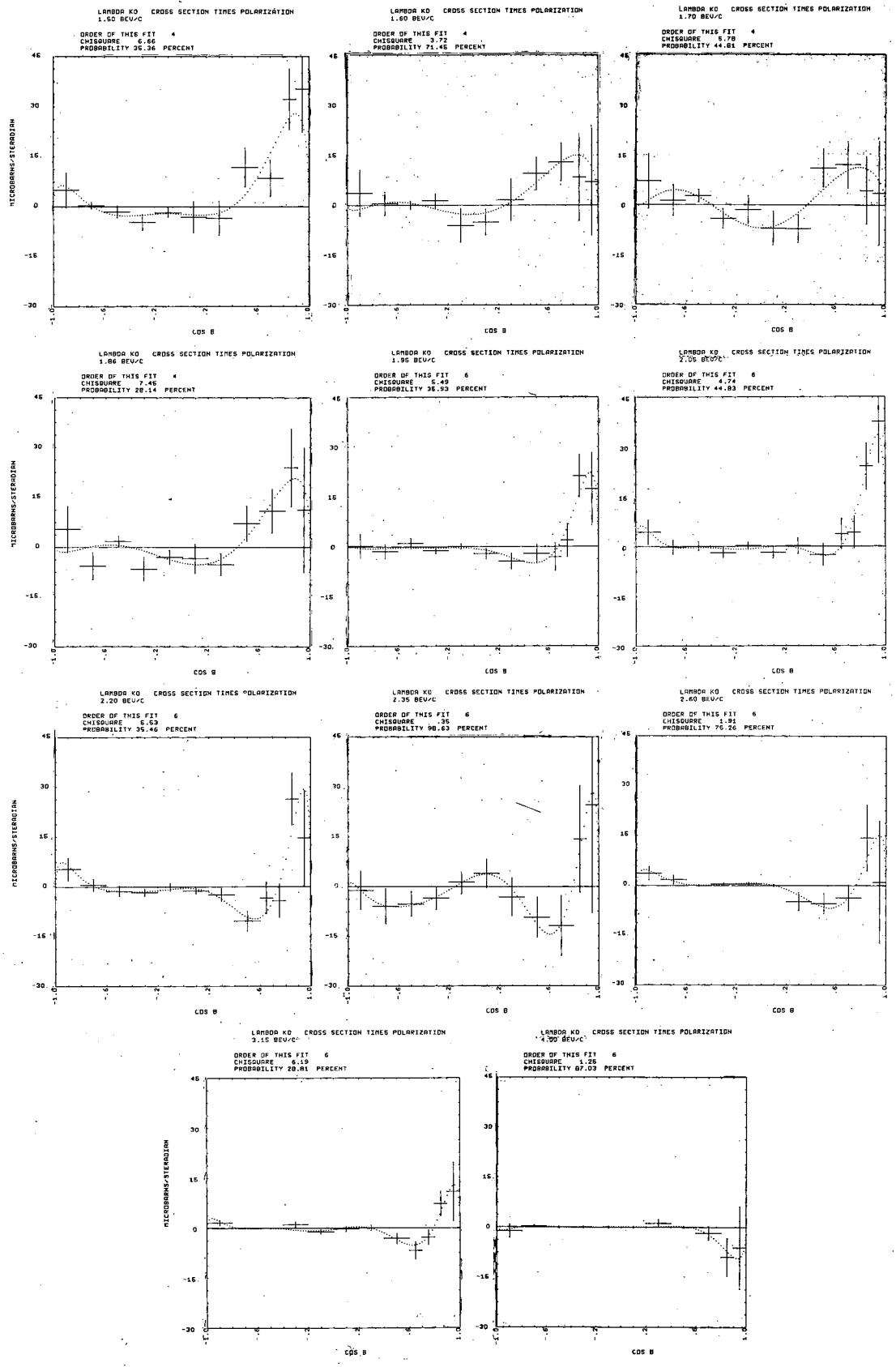

MUB 11636

Fig. 10

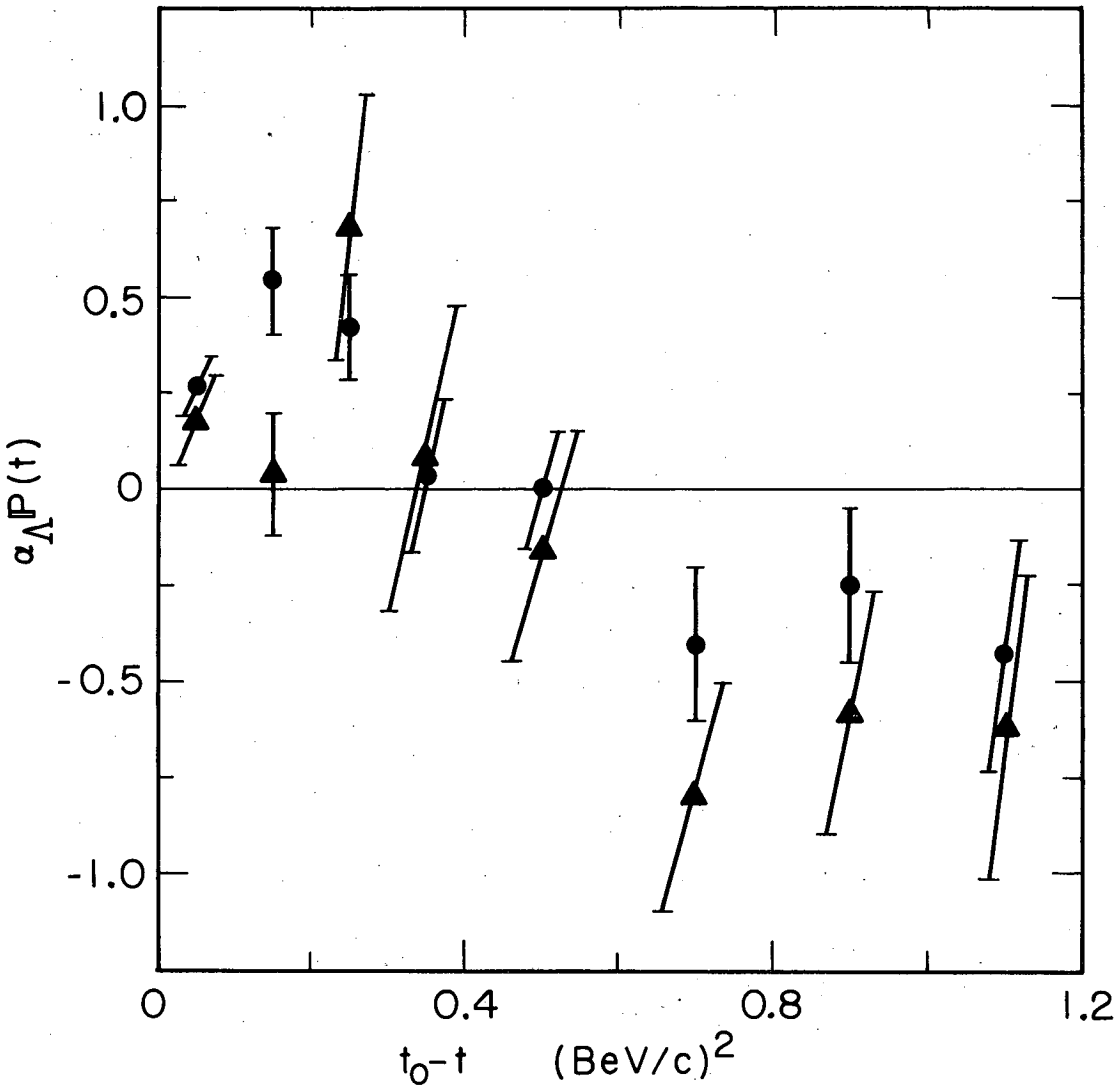

Fig. 11